Published in final edited form as:
Cancer Res. 2009 August 1; 69(15): 6021–6026. doi:10.1158/0008-5472.CAN-09-1086.

Host-Derived Tumor Endothelial Marker 8 (TEM8) Promotes the Growth of Melanoma

Mike Cullen[1,5], **Steven Seaman**[1,5], **Amit Chaudhary**[1], **Mi Young Yang**[1], **Mary Beth Hilton**[1,2], **Daniel Logsdon**[2], **Diana C. Haines**[3], **Lino Tessarollo**[4], and **Brad St. Croix**[1]

[1]Tumor Angiogenesis Section, Mouse Cancer Genetics Program (MCGP), NCI-Frederick, Frederick, MD 21702, USA

[2]Basic Research Program, SAIC, NCI-Frederick, Frederick, MD 21702, USA

[3]Pathology/Histotechnology Laboratory, SAIC, NCI-Frederick, Frederick, MD 21702, USA

[4]MCGP, NCI- Frederick, Frederick, MD 21702, USA

Abstract

TEM8 was initially identified as a gene overexpressed in the vasculature of human tumors and was subsequently identified as an anthrax toxin receptor. To assess the functional role of TEM8, we disrupted the *TEM8* gene in mice by targeted homologous recombination. TEM8$^{-/-}$ mice were viable and reached adulthood without defects in physiological angiogenesis. However, histopathologic analysis revealed an excess of extracellular matrix (ECM) in several tissues including the ovaries, uterus, skin, and periodontal ligament of the incisors, the latter resulting in dental dysplasia. When challenged with B16 melanoma, tumor growth was delayed in TEM8$^{-/-}$ mice while the growth of other tumors, such as Lewis lung carcinoma, was unaltered. These studies demonstrate that host-derived TEM8 promotes the growth of certain tumors and suggest that TEM8 antagonists may have utility in the development of new anti-cancer therapies.

The vascularization of solid tumors provides tumor cells with an essential supply of oxygen and nutrients and is considered a prerequisite for the sustained growth and spread of cancer (1). The successful design of rational new agents which can inhibit tumor growth by destroying or preventing the growth of tumor blood vessels depends on an intimate molecular understanding of tumor angiogenesis. Global analyses of gene expression of endothelial cells (ECs) lining the tumor blood vessels of human colorectal cancer has led to the identification of a series of genes called Tumor Endothelial Markers, or TEMs (2). Of these, TEM8 is of particular interest because of its overexpression in tumor vessels of multiple tumor types, cell surface localization, high conservation among species, and lack of detectable expression in the angiogenic vessels of the corpus luteum (2–4). The predominant form of TEM8 is a single-pass transmembrane glycoprotein of approximately 80 to 85-kDa containing an extracellular von Willebrand Type A (vWA) domain and a large cytoplasmic tail. In vitro TEM8 has been found to bind collagen type VI and type I (3,5,6). Both TEM8 and Capillary Morphogenesis Protein 2 (CMG2), its closest homologue, have been identified as anthrax toxin receptors, and are therefore also known as ANTXR1 and ANTXR2, respectively (7,8). Interestingly, anthrax lethal toxin, composed of lethal toxin and protective antigen, displayed potent anti-tumor activity in pre-clinical tumor models when judiciously administered to mice at non-toxic doses (9–13). Upregulation of TEM8 in tumor vessels may help to explain the tumoricidal activity

Correspondence: Brad St. Croix, E-mail: stcroix@ncifcrf.gov, Ph: 301-846-7456, Fax: 301-846-7017.
[5]These authors contributed equally

of anthrax lethal toxin in vivo, but CMG2, also expressed in ECs, could potentially play a role. To better understand the normal functional role of TEM8, we disrupted the *TEM8* gene in mice by homologous recombination. These studies show that TEM8 plays an important role in normal extracellular matrix (ECM) homeostasis and the growth of certain tumor types, such as melanoma.

Materials and Methods

See supplemental data for additional methods.

Generation of TEM8 KO mice

The TEM8 knockout strategy is described in detail in the supplemental data. TEM8 knockout mice were originally made on a mixed 129SvJae/C57BL6 genetic background and have been backcrossed more than 10 generations onto a C57BL6 background. Each of the experiments described herein were performed on mice which had been backcrossed at least 5 generations and were at least 95% C57BL6.

Endothelial purification, RT-PCR and quantitative real-time PCR (qPCR)

Purification of ECs from tumors or normal tissues, mRNA isolation, cDNA synthesis and RT-PCR or qPCR was performed as previously described (14) using rat anti-mouse CD31 antibodies (BD Pharmingen) for the EC isolation. Primers can be found in supplemental Table 1.

Histological examination

A comprehensive set of tissues from six $TEM8^{+/+}$ and eight $TEM8^{-/-}$ 6- to 8-month-old mice were fixed in formalin, routinely processed, paraffin-embedded, sectioned at 5um, stained with hematoxylin and eosin (H&E) and trichrome, and evaluated by a boarded veterinary pathologist (DH). For immunofluorescence staining, see supplemental methods.

Results and Discussion

To disrupt the *TEM8* gene in mice, a targeting vector was designed to remove the first exon of *TEM8* which contains part of the TEM8 promoter, the start codon, and the signal peptide (Fig. 1*A* and Supplementary methods). The introduction of lox-p sites into the genomic sequence upstream and downstream of exon1 allowed the removal of this exon by crossing mice with a transgenic deleter strain that constitutively expresses cre recombinase (β-actin-Cre). Genotyping of 987 offspring from $TEM8^{+/-}$ heterozygous intercrosses using a PCR assay (Fig. 1*B*) revealed $TEM8^{-/-}$ mice at the expected Mendelian frequency (Supplementary Table2). To determine if TEM8 knockout mice were able to breed, we crossed $TEM8^{-/-}$ males to $TEM8^{+/+}$ females and $TEM8^{-/-}$ females to $TEM8^{+/+}$ males. Both crossings produced a similar number of offspring, averaging 7.0 ± 1.4 ($TEM8^{+/+}$) or 6.8 ± 0.5 ($TEM8^{-/-}$) pups per litter (Supplementary Table 3). To confirm that the *TEM8* allele was deleted, we analyzed the expression of TEM8 mRNA and protein. For this, we isolated tumor ECs from TEM8 wildtype or mutant mice, because TEM8 is highly expressed in these cells (4). RT-PCR analysis of *TEM8* using PCR primer pairs downstream of the deleted exon1 revealed *TEM8* mRNA expression in tumor ECs isolated from $TEM8^{+/+}$ but not $TEM8^{-/-}$ mice (Fig 1*B*). Similarly, western blot analysis revealed TEM8 protein only in tumor ECs of TEM8 wildtype mice (Fig. 1*C*) when probed with an anti-TEM8 antibody (clone SB5) which bound to an epitope downstream of the deleted exon1 (Supplementary Fig. 1). Taken together, these studies suggest that TEM8 protein is not expressed in our $TEM8^{-/-}$ mice, and that normal growth and development is, for the most part, unaffected by loss of TEM8.

A phenotype observed in adult TEM8$^{-/-}$ mice, which became more pronounced with age, was a misalignment of their incisors (Fig. 1D). Continual growth of the incisors is normal in rodents but adult tooth size is usually controlled by interactive wear between aligned upper and lower teeth. To prevent the abnormal tooth growth from interfering with food intake, incisors of the TEM8$^{-/-}$ mice were routinely clipped. Over the course of 10 weeks, body weights of male and female TEM8$^{-/-}$ mice were similar to their sex-matched TEM8$^{+/+}$ littermates (Supplementary Fig. 2). Thus, as long as teeth were clipped, mutant mice appeared to develop normally without any other obvious behavioral or gross anatomical abnormalities.

In a further effort to identify defects in TEM8$^{-/-}$ mice, we performed a comprehensive histological analysis of adult mice. This analysis revealed mild to moderate increased ECM in several organs including the ovaries, uterus and skin (Fig. 2). In female mice, loose proteinacious ECM deposits were found throughout the ovaries, although follicles appeared to develop normally. In the uterus, increased ECM was noted in the lamina propria of the endometrium and, to a lesser extent, in the musculature. The metaphyseal periosteum of the femurs was mildly thickened due to increased ECM, and there was minimal periosteal thickening of the vertebra. Severe thickening of the periodontal ligament due to increased ECM was evident around the incisors, and to a lesser extent, around the molars. The excessive ECM in the tissues surrounding the incisors presumably leads to their misalignment which in turn results in a loss of normal abrasion and their eventual overgrowth. Associated degeneration of the enamel organ with resultant dental dysplasia was also consistent with the clinically noted incisor abnormalities. The cranial sutures of the skull were also thickened by increased ECM. More subtle increases in ECM were also noted in the lamina propria of the stomach, small and large intestines, urinary bladder, cervix and tongue. Trichrome staining of the affected tissues suggested the excessive ECM to be collagen (Fig. 2*A*, bottom panel), but an increase in the number of fibroblasts was not evident. Because TEM8 has been found to bind collagen type I and collagen type VI in vitro (3,6) we reasoned that disruption of TEM8 could potentially lead to a reduced uptake and degradation of these or other ECM proteins. Interestingly, immunofluorescence staining revealed focal deposits of collagen type I and collagen type VI in the TEM8$^{-/-}$ ovaries and uterus (Fig. 2*B* and supplemental Fig. 3*A*), but other ECM proteins such as laminin and fibrinogen showed similar patterns of staining between knockout and wildtype mice. Western blotting also revealed increased levels of both collagen type I and collagen type VI in TEM8-deficient tissues (Supplemental figure 3*B*).

We also analyzed TEM8$^{-/-}$ mice for defects in angiogenesis. First, the vessels of the developing retina, which form postnatally in rodents, were analyzed. From P0.5 to P10.5 no differences in vessel development or branching was noted in either the inner primary or outer vascular plexuses (Fig. 3*A* and data not shown). We also analyzed wound healing in adult mice, but found no differences in the rate of wound closure in TEM8$^{+/+}$ or TEM8$^{-/-}$ mice (Fig. 3*B*). Consistent with this result, immunofluorescence staining of vessels in wound sections failed to reveal differences in vessel numbers (Fig. 3*C*). We also compared angiogenesis using the mouse aortic ring assay and evaluated VEGF and FGF stimulated angiogenesis using the Directed *In vivo* Angiogenesis Assay (DIVAA) (15), but again no difference was found (data not shown). Vessel structures also appeared unaltered in the uterus (Fig. 3*D*) and ovaries, two of the tissues that displayed excess deposits of ECM.

Because TEM8 is overexpressed in tumor vessels, we reasoned that it might be important for pathological angiogenesis. To test this idea, TEM8$^{-/-}$ or TEM8$^{+/+}$ littermates were challenged subcutaneously with syngeneic Lewis lung carcinoma (LLC) or B16 melanoma tumors (Fig. 4*A*). Interestingly, B16 tumors grew slower in TEM8$^{-/-}$ compared to TEM8$^{+/+}$ mice, a result that was confirmed in four independent experiments. Although there appeared to be a slight delay in the growth of LLC tumors, the difference was not statistically significant. Thus, TEM8 expression in the host appears to preferentially promote the growth of certain tumor types.

In order to gain insight into possible mechanisms regulating the reduced B16 tumor growth in TEM8 mutant mice, we performed immunofluorescent staining of B16 tumor sections. An analysis of vessels using the endothelial marker PV-1 (Meca-32) did not reveal any differences in vessels density between $TEM8^{-/-}$ or $TEM8^{+/+}$ mice (Fig. 4*B*). Pericytes numbers were also unaltered (Fig. 4*C*). We also evaluated the number of proliferating ECs, the extent of hypoxia and the level of apoptosis in tumors but again did not identify and differences between wildtype and knockout mice (Supplemental Fig. 4). The number of host-derived inflammatory cells, such as CD68 positive macrophages, CD19 positive B-cells, CD11b positive myeloid cells and CD18 or CD45 positive leukocytes was also unchanged (data not shown).

Because B16 tumor growth appeared to depend more on host-derived TEM8 than LLC tumors, we expected that TEM8 might be expressed at a higher level in B16 tumor ECs. To address this possibility, we performed qPCR on ECs isolated from LLC or B16 tumors. The endothelial markers CD31 and VE-cadherin were highly enriched in the isolated ECs compared to unfractionated tumors (202-fold and 283-fold, respectfully), confirming their purity (Supplemental Fig. 5). Unexpectedly, TEM8 mRNA levels were approximately 4-fold higher in LLC compared to B16 tumor ECs suggesting that reduced TEM8 expression in LLC tumor ECs was not responsible for the noted differential effects on tumor growth (Fig. 4*D*). CMG2, on the other hand, was approximately 2-fold higher in cultured LLC tumor cells compared to B16 tumor cells and was approximately 2-fold higher in LLC versus B16 tumor-derived ECs. Thus, CMG2 may share functional redundancy with TEM8, potentially contributing to the subdued response to TEM8 loss noted in the LLC tumor model. A possible redundant or overlapping function is supported by the fact that both TEM8 and CMG2 are able to bind anthrax toxin proteins (7,8), both bind ECM molecules in vitro (3,5,6,16), and deletion or mutation of either of these genes leads to excessive ECM (17,18).

An important question is whether loss of TEM8 expression solely in ECs is responsible for the B16 tumor growth delay and the excess ECM observed in certain organs or if pericytes, tumor associated fibroblasts, or other host cell types are also involved. Our conditional knockout mouse should provide a valuable tool for answering this question. $TEM8^{-/-}$ mice will also provide a valuable tool for evaluating the role of TEM8 in anthrax mediated toxicity in vivo.

Interestingly, mutations in the TEM8 homologue CMG2 have been found to cause the disorders juvenile hyaline fibromatosis and infantile systemic hyalinosis (17,18). These diseases are associated with the accumulation of amorphous uncharacterized ECM. In cell culture, CMG2 has been found to bind laminin and collagen type IV while TEM8 has been found to bind collagen type I and collagen type VI (3,6,16). In vivo, we found focal overexpression of collagen type I and collagen type VI in $TEM8^{-/-}$ mice. Taken together, these results suggest that both TEM8 and CMG2 play important roles in ECM homeostasis. That TEM8 promotes the growth of certain tumors suggests that antagonism of TEM8 function may be a useful strategy for the development of new anticancer agents.

Supplementary Material

Refer to Web version on PubMed Central for supplementary material.

Acknowledgments

This research was supported by the intramural research program of the NCI, NIH, DHSS, and with federal funds from the NCI under Contract No. HHSN261200800001E. The content of this publication does not necessarily reflect the views or policies of the DHSS, nor does mention of trade names, commercial products, or organizations imply endorsement by the U.S. Government. We thank Dr. Jill Dunty for purifying SB5 antibodies, members of the MCGP for helpful discussion and Drs. Stephan H. Leppla and Shihui Liu for sharing unpublished data prior to publication.

References

1. Kerbel RS. Tumor angiogenesis. N Engl J Med 2008;358:2039–2049. [PubMed: 18463380]
2. St Croix B, Rago C, Velculescu V, et al. Genes expressed in human tumor endothelium. Science 2000;289:1197–1202. [PubMed: 10947988]
3. Nanda A, Carson-Walter EB, Seaman S, et al. TEM8 interacts with the cleaved C5 domain of collagen alpha 3(VI). Cancer Res 2004;64:817–820. [PubMed: 14871805]
4. Carson-Walter EB, Watkins DN, Nanda A, Vogelstein B, Kinzler KW, St Croix B. Cell surface tumor endothelial markers are conserved in mice and humans. Cancer Res 2001;61:6649–6655. [PubMed: 11559528]
5. Hotchkiss KA, Basile CM, Spring SC, Bonuccelli G, Lisanti MP, Terman BI. TEM8 expression stimulates endothelial cell adhesion and migration by regulating cell-matrix interactions on collagen. Exp Cell Res 2005;305:133–144. [PubMed: 15777794]
6. Werner E, Kowalczyk AP, Faundez V. Anthrax toxin receptor 1/tumor endothelium marker 8 mediates cell spreading by coupling extracellular ligands to the actin cytoskeleton. J Biol Chem 2006;281:23227–23236. [PubMed: 16762926]
7. Bradley KA, Mogridge J, Mourez M, Collier RJ, Young JA. Identification of the cellular receptor for anthrax toxin. Nature 2001;414:225–229. [PubMed: 11700562]
8. Scobie HM, Rainey GJ, Bradley KA, Young JA. Human capillary morphogenesis protein 2 functions as an anthrax toxin receptor. Proc Natl Acad Sci U S A 2003;100:5170–5174. [PubMed: 12700348]
9. Abi-Habib RJ, Singh R, Leppla SH, et al. Systemic anthrax lethal toxin therapy produces regressions of subcutaneous human melanoma tumors in athymic nude mice. Clin Cancer Res 2006;12:7437–7443. [PubMed: 17189417]
10. Rouleau C, Menon K, Boutin P, et al. The systemic administration of lethal toxin achieves a growth delay of human melanoma and neuroblastoma xenografts: assessment of receptor contribution. Int J Oncol 2008;32:739–748. [PubMed: 18360701]
11. Duesbery NS, Resau J, Webb CP, et al. Suppression of ras-mediated transformation and inhibition of tumor growth and angiogenesis by anthrax lethal factor, a proteolytic inhibitor of multiple MEK pathways. Proc Natl Acad Sci U S A 2001;98:4089–4094. [PubMed: 11259649]
12. Liu S, Aaronson H, Mitola DJ, Leppla SH, Bugge TH. Potent antitumor activity of a urokinase-activated engineered anthrax toxin. Proc Natl Acad Sci U S A 2003;100:657–662. [PubMed: 12525700]
13. Liu S, Wang H, Currie BM, et al. Matrix Metalloproteinase-activated Anthrax Lethal Toxin Demonstrates High Potency in Targeting Tumor Vasculature. J Biol Chem 2008;283:529–540. [PubMed: 17974567]
14. Seaman S, Stevens J, Yang MY, Logsdon D, Graff-Cherry C, St Croix B. Genes that distinguish physiological and pathological angiogenesis. Cancer Cell 2007;11:539–554. [PubMed: 17560335]
15. Guedez L, Rivera AM, Salloum R, et al. Quantitative assessment of angiogenic responses by the directed in vivo angiogenesis assay. Am J Pathol 2003;162:1431–1439. [PubMed: 12707026]
16. Bell SE, Mavila A, Salazar R, et al. Differential gene expression during capillary morphogenesis in 3D collagen matrices: regulated expression of genes involved in basement membrane matrix assembly, cell cycle progression, cellular differentiation and G-protein signaling. J Cell Sci 2001;114:2755–2773. [PubMed: 11683410]
17. Hanks S, Adams S, Douglas J, et al. Mutations in the gene encoding capillary morphogenesis protein 2 cause juvenile hyaline fibromatosis and infantile systemic hyalinosis. Am J Hum Genet 2003;73:791–800. [PubMed: 14508707]
18. Dowling O, Difeo A, Ramirez MC, et al. Mutations in capillary morphogenesis gene-2 result in the allelic disorders juvenile hyaline fibromatosis and infantile systemic hyalinosis. Am J Hum Genet 2003;73:957–966. [PubMed: 12973667]

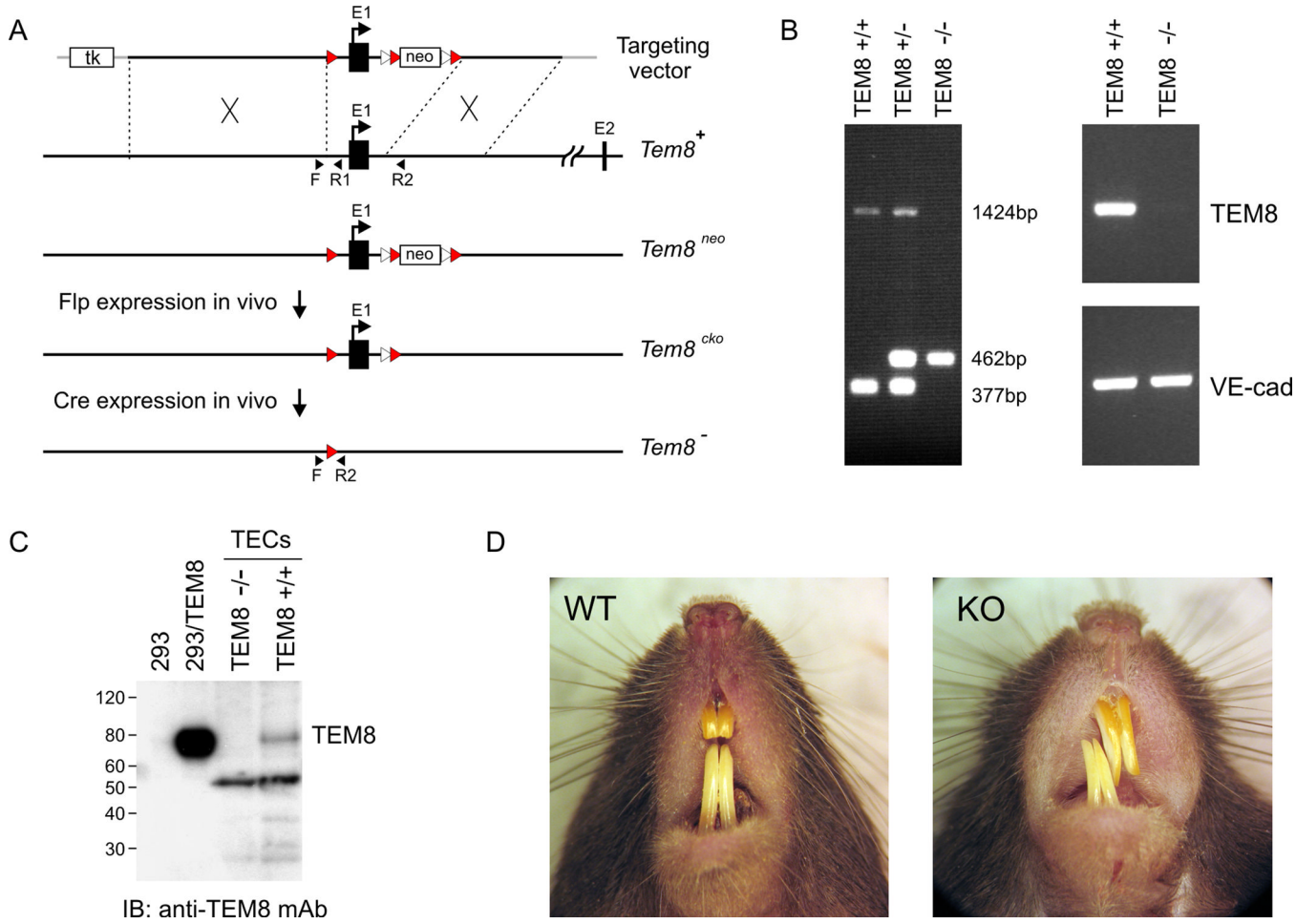

Figure 1.

Targeting vector and evidence of TEM8 loss in vivo. ***A***, A conditional *TEM8* targeting vector was generated by introducing lox-p sites (red arrowheads) into the genomic sequence upstream and downstream of exon1. Following electroporation, ES cell clones with a floxed $TEM8^{neo}$ allele were identified by southern blotting (data not shown) and used to generate chimeric mice and achieve germline transmission of the $TEM8^{neo}$ allele. $TEM8^{+/neo}$ mice were crossed with a β-actin-Cre deleter strain to generate mice with a *TEM8* null ($TEM8^{-}$) allele. Frt sites (white arrowheads) were also introduced on either side of the neomycin cassette to allow its removal with Flp recombinase generating a conditional knockout allele ($TEM8^{cko}$). Forward arrow, start codon and signal peptide; TK, thymidine kinase cassette used for negative selection; neo, neomycin cassette used for positive selection; black arrowheads indicate location of forward and reverse PCR primers used for genotyping. ***B***, *Left*, genotyping of genomic DNA by PCR. *Right*, RT-PCR was used to detect mRNA expression. Note that *TEM8* expression is only detectable in $TEM^{+/+}$ ECs derived from LLC while the endothelial marker VE-cadherin (VE-cad) is present in both samples. ***C***, An ~80kDa TEM8 protein product is detectable only in $TEM^{+/+}$ tumor-derived ECs (TECs) by immunoblotting. 293 cells stably transfected with TEM8 (293/TEM8) were used as a positive control. The band migrating at ~53kd is presumably non-specific because it was detected by the secondary antibody alone. ***D***, Incisors are misaligned in the $TEM8^{-/-}$ mice.

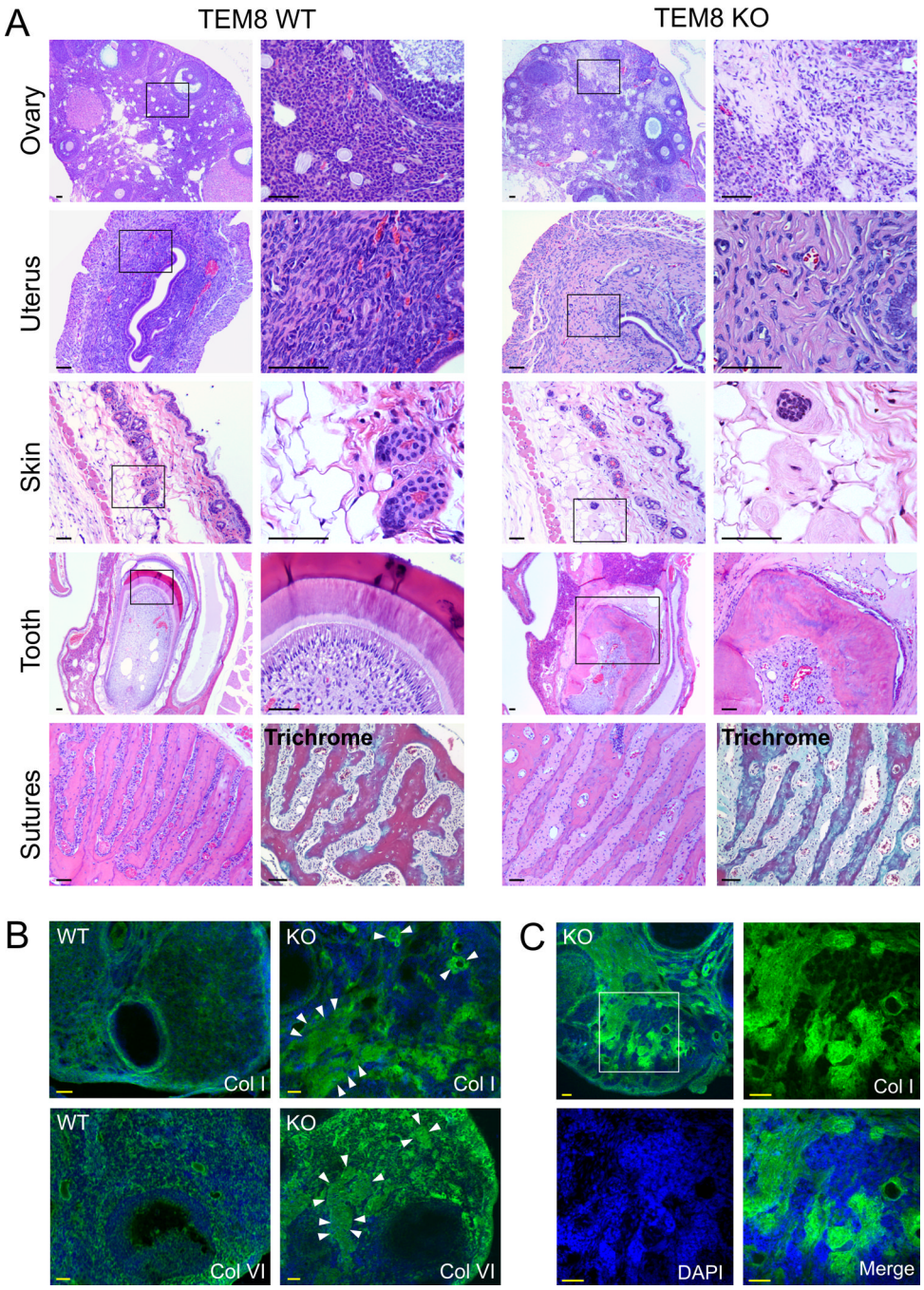

Figure 2.

Histopathologic analysis. ***A***, H&E staining of various organs. Note the increased ECM in each of the TEM8$^{-/-}$ tissues. In the skin, the excess ECM surrounded the basal aspects of the hair follicles. Periodontal thickening was most severe at the incisors, with associated degeneration of ameloblasts and odontoblasts resulting in dental dysplasia. Trichrome staining revealed the collagen-like nature of the increased ECM (cranial sutures of the skull) ***B***, Immunofluorescence staining of the ovaries revealed focal upregulation of collagen type I and type VI (green) in the TEM8$^{-/-}$ mice similar to the eosin staining in A. Arrowheads surround some of the more intensely stained pockets of collagen. ***C***, The focal patches of collagen I (FITC, green) in the

TEM8$^{-/-}$ ovaries correspond to areas of low cell density (DAPI, blue) when visualized under separate filters. Bar, 50μm.

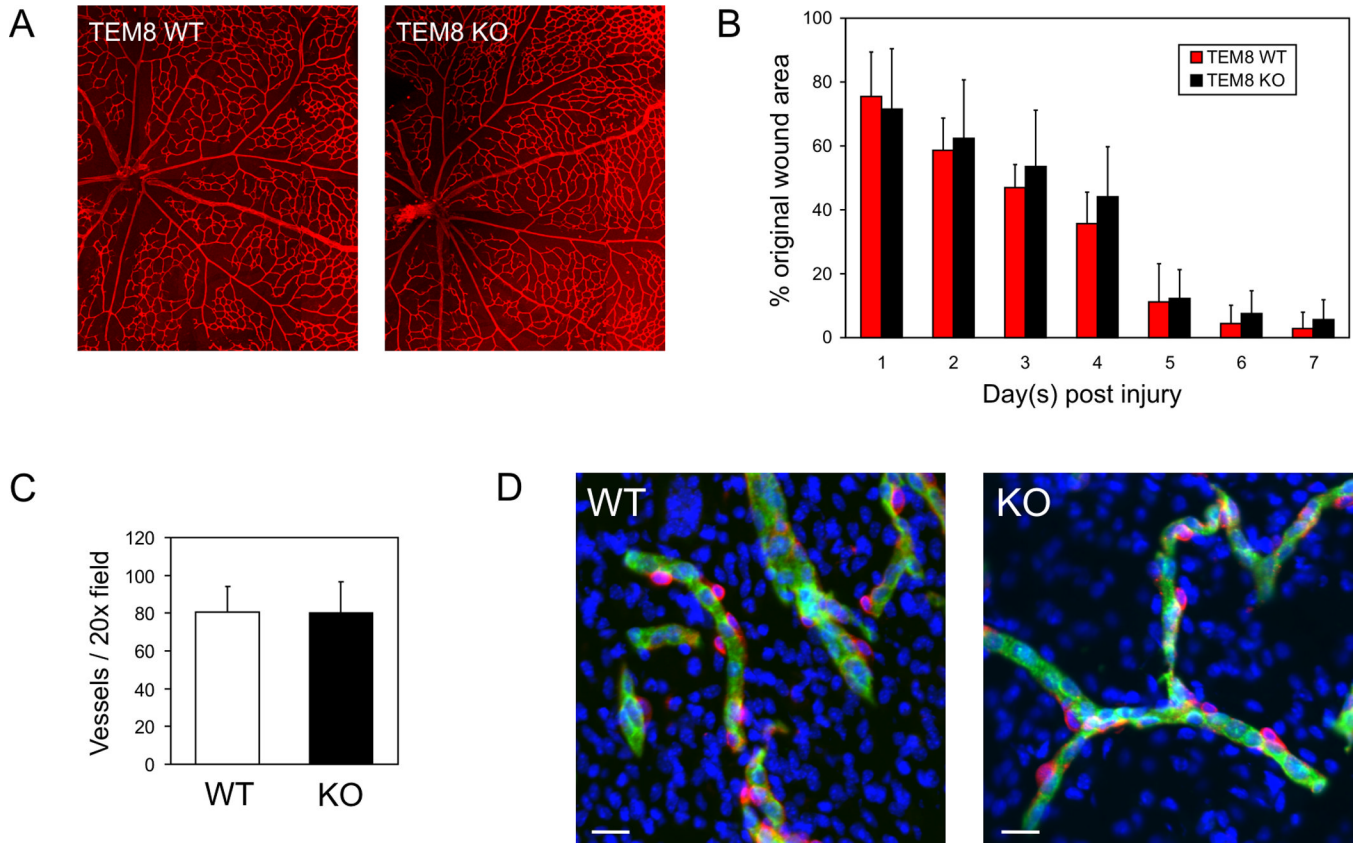

Figure 3.

Physiological angiogenesis is unaltered in TEM8$^{-/-}$ mice. Vessel structure at P10.5 in the developing retina **(A)**, the rate of wound closure **(B)**, the number of vessels in wounds **(C)** and vessel structure in the uterus **(D)** appeared similar between knockout and wildtype mice. ***D***, In the knockouts a decreased nuclear density (DAPI, blue) corresponding to areas with excessive ECM deposits (see Fig. 2) was frequently observed. CD31-positive vessels (green); NG2-positive pericytes (red). Bar, 20μm.

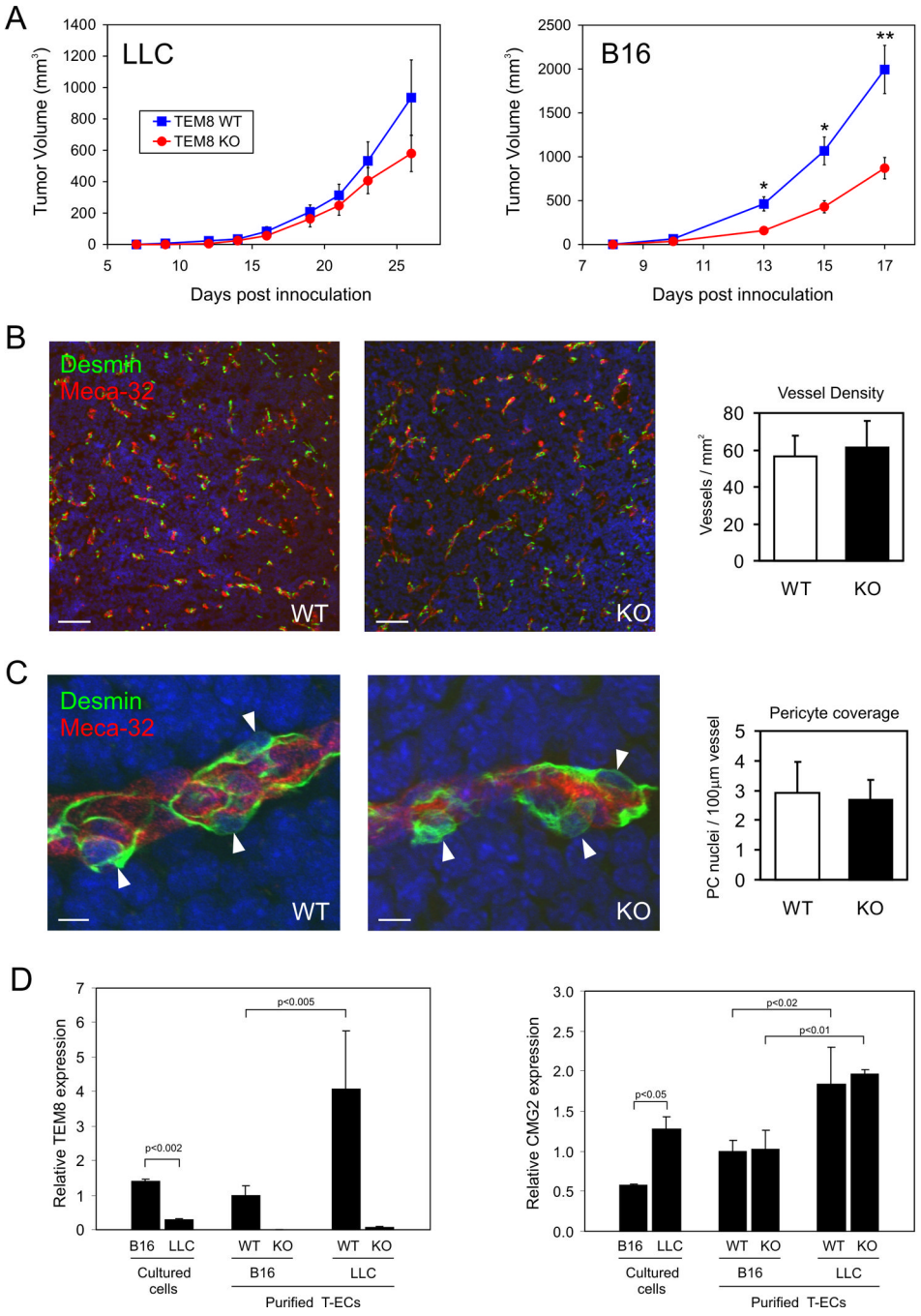

Figure 4.

Evaluation of LLC and B16 tumors in TEM8$^{+/+}$ and TEM8$^{-/-}$ mice. ***A***, Tumor growth following s.c. tumor cell injection. *n* = 6–9 for LLC; *n* = 12–13 for B16. *Points*, means; *bars*, SE; *, P < 0.005; **, P < 0.002 (student's t test). ***B***, Vessel density in B16 tumors. Immunofluorescence staining of ECs (Meca-32, red) and pericytes pericytes (Desmin, green). Bar, 100µm. ***C***, The number of pericytes in B16 tumors. Arrowheads, pericyte nuclei; Bar, 10µm. ***D***, qPCR analysis of TEM8 and CMG2 expression in B16 or LLC tumor cells in culture, or purified tumor ECs (T-ECs). Error bars represent SD derived from biological replicates (separate flasks of cultured cells or independently isolated T-EC samples).